Available online at www.sciencedirect.com
ScienceDirect
European Journal of Medicinal Chemistry 42 (2007) 614–626
EUROPEAN JOURNAL OF MEDICINAL CHEMISTRY
http://www.elsevier.com/locate/ejmech

Original article

Novel and versatile methodology for synthesis of cyclic imides and evaluation of their cytotoxic, DNA binding, apoptotic inducing activities and molecular modeling study

Alaa A.-M. Abdel-Aziz*

Department of Pharmaceutical Chemistry, College of Pharmacy, King Saud University, P.O. Box 2457, Riyadh 11451, Saudi Arabia

Received 31 May 2006; received in revised form 25 November 2006; accepted 1 December 2006
Available online 10 December 2006

Abstract

Versatile method has been developed for synthesis of *N*-substituted imides. Thus, acid anhydrides, imides and dicarboxylic acids were successfully subjected to dehydrative cyclization with substituted amines using DPPOx and Et_3N to afford *N*-substituted imides under mild conditions. The DNA binding and apoptosis induction were investigated with regard to their potential utility as cytotoxic agents. Molecular modeling methods are used to study the cytotoxic activity of the active compounds by means of molecular and quantum mechanics.

Keywords: *N*-Substituted imides; Novel synthesis; Apoptosis induction; DNA-binding; Molecular modeling

1. Introduction

Imide derivatives are a valuable group of bioactive compounds showing androgen receptor antagonists, anti-inflammatory, anxiolytic, antiviral, antibacterial, and antitumor properties [1]. In spite of their wide applicability, available procedures for their synthesis are limited [2]. Among them, the dehydrative condensation of an anhydride and an amine at high temperature [3] and the cyclization of the amic acid in the presence of acidic reagents are the typical methods of choice [4]. The direct *N*-alkylation of maleimide with alcohols under Mitsunobu reaction conditions is an alternative method for the synthesis of imide [2a]. Many catalysts including Lewis acids and hexamethyldisilazane [5] have been proposed for the synthesis of *N*-alkyl and *N*-arylimide derivatives. However, each of these routes has its own synthetic problems when applied to a range of derivatives, such as, low yields, numerous by-product formations and only a narrow range of imide derivatives can be synthesized. Moreover, microwave assisted addition of amines to phthalic anhydride has been also reported [6]. However, Westaway and Gedye [7], did not see any differences when the reaction was carried out by microwave or conventional heating in DMF. Therefore, synthesis of functionalized imides is still a challenging endeavor.

We describe herein an efficient and a mild approach for the synthesis of *N*-substituted imides from the parent imides, anhydrides and dicarboxylic acids under mild conditions. This approach requires only a few minutes of reaction time, in contrast to conventional method that requires a long reaction time and expensive Lewis acid, which is difficult to handle. We envisaged that the reaction of an anhydride with an appropriately substituted amine and subsequent in situ cyclization of the resulting amic acid in the presence of DPPOx [8] and Et_3N would give the corresponding imide derivatives which were investigated for their cytotoxic activity which may lead to tumor cell apoptosis.

2. Results and discussion

2.1. Chemistry

Activation of the carboxyl groups under mild conditions is apparently of great value as a fundamental process in a wide

* Tel.: +966 562947305; fax: +966 14676220.
E-mail address: alaa_moenes@yahoo.com

0223-5234/$ - see front matter © 2006 Elsevier Masson SAS. All rights reserved.
doi:10.1016/j.ejmech.2006.12.003

scope of chemical conversions including amide, imide and ester formations [8a]. The 5- and 6-membered heterocycles such as imidazoles, triazoles, 2-thiazolidinethiones and 2-pyridinethiol have been successfully used in the acylation and condensation reactions as the bifunctional leaving moieties [9].

In order to substantiate the concept, *N*-benzylphthalimide generated from phthalimide and benzylamine in a MeCN solution was heated at 40 °C with an equimolar amounts of benzylamine, Et_3N and diphenyl 2-oxo-3-oxazolinylphosphonate [DPPOx] for 60 min to afford the corresponding *N*-substituted imide derivatives (Table 1). This favorable result encouraged us to further improve the efficiency of the reaction to get high yields of imide derivatives in a short reaction time. In order to optimize the reaction conditions, we briefly investigated the stoichiometric ratio of the reagents and reactants. The imides' formation was observed almost quantitatively in 0.25–1 h, stirring in MeCN with equimolar amounts of an anhydride or imide and an amine, whereas the molar ratios of Et_3N and DPPOx showed a significant influence on the reaction time and the yield of imides. Although, theoretically, 1 mol equiv of Et_3N seems to be sufficient to complete the reaction, practically the isolated yield of imides was higher using 1.5 mol equiv of Et_3N and 1.5 equiv of DPPOx. When the reaction was carried out with an excess amount of Et_3N (>1.5 equiv) and/ or DPPOx (>1.5 equiv), the yield of the imides was reduced drastically and formation of undesired products was observed upon prolonged heating. In the presence of less than an equimolar quantity of Et_3N or DPPOx, the reaction was not completed even after long reaction time. The imides' formation was not observed even in a trace amount in the absence of either DPPOx or Et_3N.

Such a cyclizing condensation of phthalimide and benzylamine promoted by DPPOx–Et_3N was also observed for the reaction of phthalic anhydride or phthalic acid. The phthalic anhydride was smoothly converted to the corresponding *N*-benzylphthalimide with nearly quantitative yield when the reaction proceeded at 40 °C for 15–30 min (Table 1, entries 9 and 10). On the other hand, the reaction of phthalic acid with benzylamine gave good yield after increasing the reaction temperature to 60 °C for 45 min using 2.0 mol equiv of both Et_3N and DPPOx (Table 1, entries 11–13). Moreover, other bases such as diisopropylethylamine, DABCO, HMDS and dimethylamiopyridine were ineffective for accelerating the reaction to get high yields (Table 1, footnote). There seems to be little relationship between the accelerating effect and basic properties of working base. Furthermore, the nature of the solvent also affected the reaction yield. However, the reactions proceeded in the presence of solvents, such as THF and DMF afforded moderate yields (Table 1, entries 1–4) while the result of the reaction in toluene and benzene (Table 1, entries 7 and 8) was completely ineffective to accelerate the reaction yield, in contrast to the reaction proceeded in MeCN which gave *N*-benzylphthalimide exclusively (Table 1, entries 5 and 6).

To generalize the scope and limitations of DPPOx and Et_3N promoted imides synthesis, the reaction was examined with various structurally diverse amines and anhydrides or imides. These results are summarized in Table 2. In most cases, the amic acid ester cyclization (Fig. 1) proceeded smoothly with 1.5 mol equiv of DPPOx and 1.5 mol equiv of Et_3N in hot MeCN, giving good to excellent yields of the desired bicyclo[2.2.2]-oct-5-ene-2,3-dicarboximides **1**, 2,3-pyrazinedicarboximides **2**, 2,3-pyridinedicarboximides **3**, or phthalimides **4** (Table 2). Yields of imides derived from an anhydride or imide and an alkylamine or arylalkylamine, such as ethylamine, *tert*-butylamine, phenethylamine and benzylamine were found to be better than an aromatic amine such as aniline which may be attributed to the lower nucleophilicity of aromatic amines (Table 2, entries 1–10 vs 11–13). Generally, high yield was observed when less hindered primary amines were used which decreased when sterically congested amines were investigated (Table 2, entries 1–11 vs 12 and 13). Apparently, structural variation in the arylamine in *o*-position with steric bulky group affecting the yields of the product, such as aniline and *p*-pentylaniline (Table 2, entries 11 and 14) gave higher yield than *o*,*o*-dimethylaniline (Table 2, entry 12). However, increasing the bulkiness of *o*-position from 2,6-dimethyl to 2,6-diisopropylaniline may induce a tremendous effect on the reaction

Table 1
DPPOx promoted the synthesis of *N*-benzylphthalimide by varying solvents, bases and reaction time

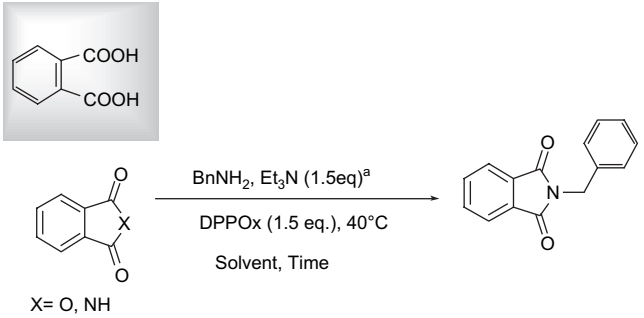

Entry	Acid	Time (min)	Solvent	Yield (%)[b]
1		60	THF	40
2		120	THF	53
3		30	DMF	61
4		60	DMF	67
5		20	MeCN	94
6		30	MeCN	95
7		120	Toluene	33
8		180	Benzene	27
9		15	MeCN	97
10		30	MeCN	98
11		30	MeCN	50
12[c]		30	MeCN	71
13[c]		45	MeCN	75

[a]Lower yields have been observed using bases other than Et_3N, such as, diisopropylethylamine (60%), HMDS (44%), Dimethylaminopyridine (52%), DABCO (33%).
[b] Isolated yields.
[c] The reaction temperature was 60 °C.

Table 2
DPPOx and Et_3N promoted synthesis of *N*-substituted imide derivatives from anhydrides or acid imides using various amines

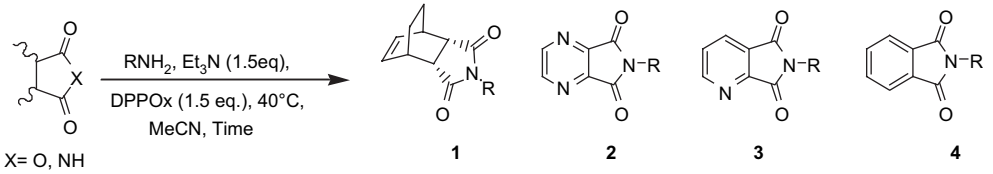

R= Et (**a**), t-But (**b**), 1-adamantyl (**c**), Phenethyl (**d**), Benzyl (**e**), 4-methoxyBenzyl (**f**), 3,4-dimethoxybenzyl (**g**), 4-chloroBenzyl (**h**), (*R*)-α-Methylbenzyl (**i**), (*S*)-α-Methylbenzyl (**j**), Phenyl (**k**), 2,6-Dimethylphenyl (**l**), 2,6-Diisopropylphenyl (**m**), 4-pentylphenyl (**n**), 4-chlorophenyl (**o**), 4-trifluoromethylphenyl (**p**)

Entry	Anhydride	Time (min)[a]	Imide	Yields (%)[b]	Entry	Anhydride	Time (min)[a]	Imide	Yields (%)[b]
1		15	**1a**	98	28		45 (45)	**2l**	74 (75)
2		20	**1b**	94	29		45 (45)	**2m**	65 (62)
3		30	**1c**	93	30		15 (30)	**2n**	93 (89)
4		15	**1d**	99	31		20 (30)	**2o**	86 (82)
5		15	**1e**	96	32		30 (45)	**2p**	83 (84)
6	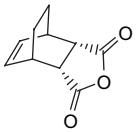	20	**1f**	97	33	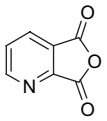	15 (30)	**3a**	99 (96)
7		15	**1g**	95	34		15 (30)	**3b**	93 (89)
8		30	**1h**	93	35		20 (30)	**3c**	89 (85)
9		30	**1i**	91	36		15 (30)	**3d**	96 (94)
10		30	**1j**	90	37		15 (30)	**3e**	95 (95)
11		30	**1k**	89	38		20 (45)	**3f**	92 (93)
12		45	**1l**	76	39		20 (45)	**3g**	90 (88)
13		45	**1m**	67	40		30 (45)	**3h**	91 (86)
14		20	**1n**	95	41		30 (30)	**3i**	89 (88)
15		30	**1o**	87	42		30 (30)	**3j**	91 (92)
16		30	**1p**	85	43		30 (45)	**3k**	87 (85)
17	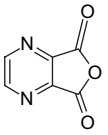	20 (30)	**2a**	96 (93)	44		45 (45)	**3l**	70 (71)
18		30 (45)	**2b**	91 (90)	45		45 (45)	**3m**	61 (60)
19		30 (45)	**2c**	87 (83)	46		15 (30)	**3n**	91 (87)
20		15 (30)	**2d**	97 (95)	47		30 (30)	**3o**	86 (85)
21		15 (30)	**2e**	96 (97)	48		30 (30)	**3p**	84 (82)
22		20 (45)	**2f**	94 (91)	49	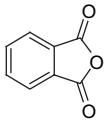	20 (30)	**4c**	92 (90)
23		20 (45)	**2g**	95 (94)	50		15 (30)	**4d**	98 (99)
24		30 (45)	**2h**	92 (89)	51		15 (20)	**4e**	97 (94)
25		30 (45)	**2i**	93 (89)	52		15 (30)	**4i**	93 (92)
26		30 (45)	**2j**	94 (93)	53		30 (45)	**4k**	91 (91)
27		30 (45)	**2k**	90 (88)	54		30 (45)	**4m**	74 (69)

[a] Time in parentheses was the reaction time using acid imides.
[b] Yield in parentheses was the isolated yield using acid imides.

products (Table 2, entry 13). It is clear that the *o*-substituents could significantly affect the amic acid ester formation which might play a crucial role in condensation step. Moreover, the presence of an electron-withdrawing group in an arylamine, such as a chloro or trifluoromethyl group leads to a decrease in the yield, compared to an arylamine containing an electron-donating group, which may be attributable to its poor nucleophilic character (Table 2, entries 14–16). When chiral amines such as (+)-(*R*)-α-methylbenzylamine or (−)-(*S*)-α-methylbenzylamine were used, the corresponding imide derivatives were isolated

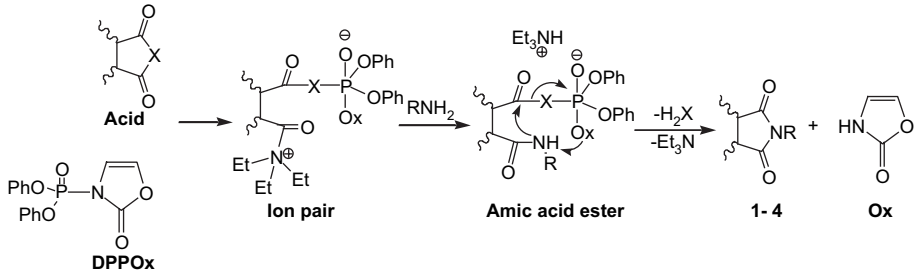

Fig. 1. Plausible mechanism of DPPOx−Et_3N promoted *N*-substituted imides formation.

without racemization under the described reaction conditions (Table 2, entries 9, 10, 25, 26, 41 and 42). It is clear from Table 2, the nature of starting acid anhydride or imide did not affect the reaction yields such as the nonplanar bicyclo[2.2.2]-oct-5-ene-2,3-dicarboxylic acid anhydride (Table 2, entries 1–16) gave nearly similar results with other planar acid anhydride including the 2,3-pyrazinedicarboxylic anhydride (Table 2, entries 17–32), 2,3-pyridinedicarboxylic anhydride (Table 2, entries 33–48) and finally phthalic anhydride (Table 2, entries 49–54).

The plausible mechanism of the direct formation of imides may involve the coupling in a concerted manner through pentavalent phosphorus ion pair and amic acid ester formation as depicted in Fig. 1. We believe that the DPPOx–Et_3N promoted formation of *N*-substituted imide could function by the reaction with acid anhydride or imide to generate a pentavalent phosphorus ion pair [8]. The ion pair is attacked by a substituted amine to afford the corresponding amic acid ester via a nucleophilic substitution. This amic acid ester can undergo intramolecular nucleophilic substitution to afford the corresponding *N*-substituted imide, oxazolone and H_2O or NH_3 (in case of acid imide). Moreover, the direct formation of an imide from phthalic acid may involve the activation through phthalic anhydride intermediate followed by amic acid ester formation as described above [8].

2.2. Biological assays

2.2.1. Cytotoxic activity

Cultured mammalian cells have been utilized recently to determine the response of the tumor cells isolated from cancer patients to various chemotherapeutic [10] agents with very high sensitivity (concentration as low as 0.25–1.7 μM). Mammalian cell culture systems have the benefit to be faster, less expensive and more sensitive than using the intact animals. Cytotoxicity assay of the prepared compounds expressed in IC_{50} values (Table 3) revealed that compounds **1c**, **1l–1n**, **2c**, **2l–2n**, **2c**, **3l–3n**, **4c** and **4m** proved to be the most active compounds in this investigation with IC_{50} values in the range of 23–10 μM. Compounds **1b**, **1h–1j** and **2b** showed moderate inhibition activity with IC_{50} values of 27, 51, 43, 49 and 32 μM, respectively; while other compounds showed weak activities.

2.2.2. DNA as an affinity probe for evaluation of biologically active compounds

DNA is the pharmacologic target of many drugs currently in clinical use or in advanced clinical trials. Small molecules that bind genomic DNA have proven to be effective anticancer, antibiotic, and antiviral therapeutic agents. It is known that small molecules can bind to DNA through various modes of interaction. They are (i) minor groove binding, (ii) major groove binding, (iii) intercalation (between two base pairs) and (iv) surface binding [11]. A variety of methods have been utilized for studying the interaction of small molecular weight compounds with DNA, such as equilibrium dialysis [12].

Briefly [13], a fixed amount of ligand is spotted on the RP-18 TLC plates followed by the addition of known amount of DNA on the same spot. The plate was then developed and the position of the DNA was determined by spraying the plates with anisaldehyde reagent. It is important to establish if the response of the test system is dependent on the dose of the test substance. In the presence of increasing quantities of DNA intercalators, a greater portion of DNA is bound to form a complex, and consequently, the free DNA was detected as a blue spot (R_f; MeOH–H_2O, 8:2) on RP-18 TLC after spraying with anisaldehyde reagent. On the other hand, compounds with high binding affinity for DNA retained on the base line. However, when the DNA was mixed with compounds with which it is known to interact (ethidium bromide), the complex was retained at the origin when MeOH–H_2O (8:2) was used for elution. Inactive compounds did not cause the DNA to be retained at the origin.

Moreover, methyl green reversibly binds polymerised DNA forming a stable complex at neutral pH. The maximum absorption for the DNA/methyl green complex is 642–645 nm. Incubation for 24 h, in the buffer used for displacement reactions in

Table 3
Cytotoxic activities of the *N*-substituted cyclic imides (μM) against Vero African green monkey kidney cells

Compound	IC_{50}	Compound	IC_{50}	Compound	IC_{50}	Compound	IC_{50}
1a	>100	**2a**	>100	**3a**	>100	**4c**	20
1b	27	**2b**	32	**3b**	33	**4d**	100
1c	14	**2c**	18	**3c**	18	**4e**	100
1d	87	**2d**	>100	**3d**	>100	**4j**	>100
1e	74	**2e**	>100	**3e**	>100	**4k**	82
1f	67	**2f**	>100	**3f**	>100	**4m**	23
1g	63	**2g**	>100	**3g**	>100	5-Fluorouracil	0.2
1h	51	**2h**	88	**3h**	95		
1i	43	**2i**	79	**3i**	81		
1j	49	**2j**	85	**3j**	92		
1k	67	**2k**	71	**3k**	72		
1l	13	**2l**	18	**3l**	20		
1m	16	**2m**	20	**3m**	21		
1n	10	**2n**	16	**3n**	18		
1o	77	**2o**	86	**3o**	92		
1p	75	**2p**	80	**3p**	87		

this study, resulted in virtually a complete loss of methyl green absorbance. This colorimetric assay [14] was used to measure the displacement of methyl green from DNA by compounds having ability to bind with DNA. The degree of displacement was determined spectrophotometrically by measuring the change in the initial absorbance of the DNA/methyl green solution in the presence of reference compound.

Results from DNA binding assay revealed that compounds **1n**, **2n**, **3n**, **1l**, **2l**, **3l** and **1c** showed the highest affinity for DNA, which was demonstrated by retaining the complex at the origin or by migrating for a very short distances, and by measuring C_{50} (concentration required for 50% decrease in the initial absorbance of the DNA/methyl green solution). Compounds **1d**, **1e**, and **2d** showed moderate activity while compounds **1a**, **2a**, **3a**, **1b**, **2b**, **3b** and **1g** showed weak activity.

2.2.3. Apoptosis assay

Progressive elucidation of the molecular mechanisms involved in cancer has opened up a new horizon for the development of new antitumor compounds. Apoptosis or programmed cell death is the prevalent mechanism complementary to proliferation that is critical for the normal development and function of multicellular organisms. Rapid proliferation needs to be balanced by apoptosis to maintain a constant cell number. Retarded cell death contributes to a wide variety of human cancers [15]. Apoptotic pathways might be significantly altered in cancer cells with respect to untransformed cells, and these differences might present a therapeutic window that can be exploited for the development of cancer drugs [16]. In contrast to necrosis, this tightly regulated and complex process exhibits some typical morphological changes, such as chromatin condensation, membrane blebbing, formation of apoptotic bodies, and in most cases, DNA fragmentation [17].

As mentioned above, development of drugs that can effectively trigger apoptosis in cancer cells has been receiving considerable attention [15h]. It is a well-known fact that the regulating mechanisms of apoptosis are extremely complex, but it is also known that the way in which the apoptotic processes function differs, depending on whether the cells involved are tumoral or healthy. These differences are due to the fact that the tumoral lines are more sensitive when these mechanisms are activated, while the healthy cells possess the ability to make repairs, which often counteracts this apoptotic process, maintaining survival of the cell [18].

However, all active compounds, subjected to cytotoxic assay, have been subjected to apoptosis methodology for studying the mechanism of cytotoxic activity using blood neutrophils and compared with positive control quercetin (Table 4). The data revealed that the human neutrophils derived from a peripheral blood of normal subjects in culture undergo morphological and chromatin fragmentation changes of programmed cell death. Moreover, the cytotoxic activities were correlated to apoptotic mechanism as indicated by the results obtained in Table 4.

2.3. Quantitative structure–activity relationship

The obtained cytotoxic results revealed that (Table 3), in the nonplanar (T-shaped imides) series (**1a**–**1p**), the *N*-ethyl **1a**, *N*-phenethyl **1d** and *N*-benzyl **1e** moieties were the least active as evidenced by their IC_{50} values of >100, 87 and 74 μM, respectively. Introduction of one or two methoxy groups and even a chloro moiety in the benzyl group resulted in a slight increase in the cytotoxic activity. Moreover, the replacement of one hydrogen atom from the α-carbon of benzyl group with a methyl moiety lead to a sharp increase of activity

Table 4
The effects of the active compounds on the apoptosis of peripheral blood neutrophils

Compound	IC_{50}[a]	Apoptotic neutrophils[b] (%)			
		0 h	24 h	48 h	72 h
1b	27	0.31 ± 0.12	12.82 ± 0.51	29.76 ± 0.04	35.64 ± 0.06
1c	14	0.89 ± 0.23	35.5 ± 0.42	5321 ± 0.28	68.11 ± 2.29
1l	13	0.92 ± 0.20	38.40 ± 0.20	5322 ± 0.2	67.98 ± 1.20
1m	16	0.87 ± 0.10	32.40 ± 0.50	49.11 ± 0.80	59.20 ± 1.40
1n	10	0.95 ± 0.04	39.11 ± 0.01	58.06 ± 0.02	70.01 ± 1.30
2b	32	0.32 ± 0.13	12.00 ± 0.2	27.60 ± 0.05	33.91 ± 0.60
2c	18	0.72 ± 0.10	30.01 ± 0.13	45.10 ± 0.11	54.05 ± 0.02
2l	18	0.65 ± 0.23	28.00 ± 0.34	42.03 ± 0.10	50.10 ± 0.10
2m	20	0.44 ± 0.10	24.07 ± 0.09	38.10 ± 0.20	46.11 ± 0.03
2n	16	0.77 ± 0.30	31.10 ± 0.10	4920 ± 0.03	60.00 ± 1.10
3b	33	0.36 ± 0.02	11.00 ± 0.30	25.07 ± 0.21	30.23 ± 0.03
3c	18	0.80 ± 0.10	31.10 ± 0.23	46.00 ± 0.04	56.10 ± 0.70
31	20	0.39 ± 0.01	22.21 ± 0.31	35.00 ± 0.24	44.16 ± 0.30
3m	21	0.36 ± 0.21	19.10 ± 0.33	32.77 ± 0.24	41.62 ± 0.50
3n	18	0.69 ± 0.03	32.11 ± 0.01	47.05 ± 0.11	57.87 ± 1.10
4c	20	0.37 ± 0.20	21.11 ± 0.23	34.66 ± 0.31	42.01 ± 0.21
4m	23	0.34 ± 0.23	15.56 ± 0.04	3021 ± 0.04	39.10 ± 0.03
DMSO	nd[c]	0.37 ± 0.01	0.39 ± 0.01	0.39 ± 0.01	0.36 ± 0.01
Quercetin	nd[c]	0.88 ± 0.03	39.90 ± 0.02	49.90 ± 0.02	71.30 ± 0.07

[a] Data was taken from Table 3.
[b] Values represent the percentage of apoptotic neutrophils (mean ± SD, $n = 3$–5 separate determinations).
[c] No data available.

as indicated by their IC_{50} (**1i**; 43 μM, **1j**; 49 μM vs **1e**; 74 μM). Replacement of *N*-ethyl moiety with the corresponding *N*-*tert*-butyl **1b** or *N*-(1-adamantyl) **1c** analogue resulted in controversial values of inhibition with IC_{50} values of 27 μM and 14 μM, respectively. In the *N*-phenyl series, introduction of an electron-donating functional group resulted in a sharp increase in activity by 6-fold (**1l**; 13 μM, **1m**; 16 μM and **1n**; 10 μM vs **1k**; 67 μM); while introduction of an electron-withdrawing group lead to a decrease in activity as indicated by their IC_{50} (**1o**; 77 μM and **1p**; 75 μM vs **1k**; 67 μM). Replacing the T-shaped imides (structure **1**) with the planar form such as series **2**, **3** or **4** decreased the activity such as IC_{50} values of **2c**, **3c**, and **4c** were 18 μM, 18 μM and 20 μM, respectively, while IC_{50} value of compound **1c** was 14 μM. It is obvious from the structure–activity profile of *N*-substituted imides that substituents with steric bulky 1-adamantyl moiety or aryl groups greatly influence the cytotoxic activity (Table 3). Apparently, a small structural variation in the *N*-substituted imides may induce a tremendous effect on cytotoxic activity. It is noteworthy that the observed cytotoxic activity was highly dependent on the bulkiness of the *N*-aryl substituents on the imide core, in which *ortho*-disubstituents played an important role in achieving an excellent level of cytotoxic activity indicating that the steric bulk of the substituents played a critical role in the cytotoxic enhancing activity. The 1-adamantyl, 2,6-dimethylphenyl and 4-*n*-pentylphenyl groups represent the *N*-substituents of choice for expressing significant activity, such as compounds **1c**, **1l**, **1n** and their analogues in series **2** and **3** which were five times more active than the phenyl derivatives **1k**, **2k** and **3k** and 10-fold more active than the less bulky ethyl and arylalkyl derivatives **1a**, **2a** and **3a**.

The results of the DNA binding assay revealed that compounds **1n**, **2n**, **3n**, **1l**, **2l**, **3l** and **1c** exhibited marked affinity for DNA as indicated by their concentration required for 50% decrease in the initial absorbance of the DNA/methyl green solution (31, 42, 49, 53, 59, 64, 69 μg/ml, respectively). Moreover, low levels of DNA binding affinity were achieved for **1d** (75 μg/ml) and **1e** (77 μg/ml), while compound **1a** showed weak activity (90 μg/ml). The obtained results might suggest that DNA binding is partially correlated with the cytotoxic activity of target compounds (Table 3). It would appear that affinity for DNA is not the sole determinant of cytotoxic potency in this series of compounds. The existence of a dual mechanism is possible whereby DNA binding contributes as one mechanism only.

The obtained apoptotic testing results (Table 4), for the most active cytotoxic compounds along with value obtained for quercetin, the reference substance, showed that compounds **1c**, **1l**–**1n**, **2c**, **2l**, **2n**, **3c** and **3n** achieved significant apoptosis levels as indicated by their percentages for inducing apoptosis in blood neutrophils after 72 h (68.1, 67.9, 59.2, 70.0, 54.0, 50.1, 60.0, 56.1, 57.8, respectively). Furthermore, good levels of apoptosis induction were achieved for **2m** (46.1), **3l** (44.1), **3m** (41.6) and **4c** (42.0) in this cell line after 72 h. With regard to the obtained results in Table 4, there is a quite correlation between the cytotoxic activity and apoptotic inducing ability.

2.4. Molecular modeling study

An attempt to gain a better insight on the molecular structures of the active compounds **1c**, **1l**, **1n**, **2c**, **2l** and **2n** and nonactive compounds **1d** and **1e**, conformational analysis of the target compounds has been performed by use of the MM+ [19] force-field (calculations in vacuo, bond dipole option for electrostatics, Polak–Ribiere algorithm, and RMS gradient of 0.01 kcal/Å mol) as implemented in HyperChem 5.1 [20]. As clear from the calculation, most of the target compounds exhibit structural similarity as indicated by their molecular parameters (Table 5). The results show that compounds **1d** and **1e** exhibited the same arrangement of the aryl groups around the imide core showing two main conformers *syn* and *anti* in which the aryl moiety was deviated from the planar imide core by −88 to −94° in case of *syn*-conformer and by 89–102° in case of *anti*-conformer (Fig. 2). The lower activity of such compounds may be attributed to the occurrence of these two conformers caused by low barrier of

Table 5
Molecular parameters of the active compounds compared with nonactive one

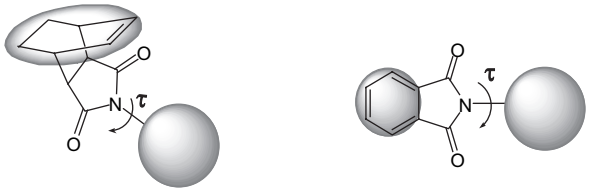

Compound	Log *P*[a]	MV[b]	MSA[c]	R[d]	Plane angle[e] (τ°)	IC_{50}[f]
1b	1.3	704	417	65.8	59.9	27
1c	2.2	870	497	87.1	59.9	14
1l	3.1	806	469	82.6	91.4	13
1m	4.6	971	537	101.1	81.6	16
1n	4.2	1006	599	95.1	90.0	10
2b	0.9	592	370	52.4	57.9	32
2c	1.8	754	449	73.7	60.4	18
2l	2.7	707	428	69.2	94.9	18
2m	4.2	891	518	87.9	88.6	20
2n	3.8	892	549	81.7	87.1	16
3b	1.4	601	373	54.8	57.1	33
3c	2.3	765	453	76.1	60.3	18
3l	3.2	717	434	71.7	95.1	20
3m	4.6	901	522	90.4	88.7	21
3n	4.3	902	551	84.2	87.2	18
4c	2.7	774	456	78.6	60.2	20
4m	5.1	912	526	92.9	88.7	23
1a	0.8	628	387	56.5	89.3 (−87.5)[g]	>100
1d	2.5	845	508	80.8	89.3 (−88.3)[g]	87
1e	2.3	786	471	76.2	102.9 (−94)[g]	74

[a] Partition coefficient.
[b] Molecular volume.
[c] Molecular surface area.
[d] Refractometry.
[e] Torsional angle between the plane of the imide ring and *N*-substituent group.
[f] Data was taken from Table 3.
[g] Torsional angle of the *syn*-conformer.

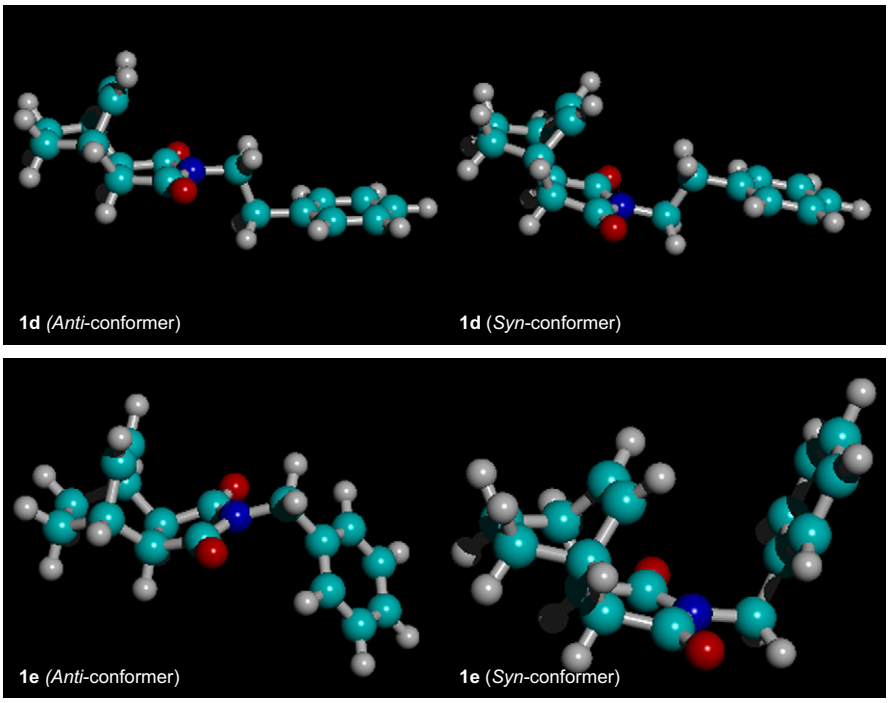

Fig. 2. Lowest energy conformers of the selected nonactive compounds **1d** and **1e** with balls and cylinders rendering (*anti* and *syn* conformers).

rotations, which were lower than 1 kcal/mol. Both conformers of compound **1d** or **1e** can exist. On the contrary, the more active compounds showed only one conformer in which the *N*-substituent group was deviated from the imide core by 57–60° in case of aliphatic substituent group such as *tert*-butyl or 1-adamantyl (Fig. 3, Table 5; **1b**, **1c**, **2b**, **2c**, **3b**, **3c** and **4c**) and 81–95° in case of *N*-aryl derivatives such as compounds **1l**, **1m**, **1n**, **2l**, **2m**, **2n**, **3l**, **3m** and **3n** (Table 5). As evident from the experimental data, the structural features (pharmacophore) essential for the cytotoxic activity of this series are as follows; (i) nonplanar imide core is more favorable for the best activity, (ii) the presence of a hydrophobic aryl moiety directly attached to imide backbone enhances the activity, (iii) this aryl group adapts only one conformer which may be responsible for the activity, in contrary to benzyl moiety, (iv) the presence of steric bulky *o*,*o*-dialkyl or *p*-pentyl groups in the aromatic group or its steric equivalent 1-adamantyl is necessary for the activity, (v) the steric and hydrophobic parameters are essential factors affecting the activity as indicated by the experimental and theoretical data (Fig. 3, Table 5). The stable conformers resulting from computational chemistry analysis as a representative example were superimposed in order to reveal the similarities and differences in structure (Fig. 4). The strategy of overlay fit was to match imide rings and to examine any spatial differences between the atoms of the *N*-substituent groups. The results show that atoms of the aryl groups occupy slightly different spatial position relative to the plane of imide core. Further evidence for identical biological activity [21] comes from QSAR data that were derived from the QSAR module of HyperChem using the conformations depicted in Figs. 2 and 3. As a result, the QSAR displays calculated data for ClogP (the hydrophobic parameters), refractivity (steric and polarizability parameters), molecular volume (steric and polarizability parameters), grid surface area (Table 5) [22]. Despite a variation of the molecular shape of the active compounds, measurements of global molecular parameters (surface area, volume, and refractivity) reflect their similarity. As can be shown, ClogP values of the most active compounds are well in the range of 2.7–4.6 while for compounds **1c** and **2c**, ClogP values are somewhat lower i.e. 2.2 and 1.8, respectively, so the optimum hydrophobicity of the active compounds is close to 2.0–5.1. However, direct correlation could be established between the ClogP and cytotoxic activity of the series as indicated by their IC_{50} values (Table 5), such as the ClogP values of **1a** (0.8), **1b** (1.3), **1c** (2.2), **1l** (3.1) and **1n** (4.2) are well correlated with their cytotoxicity (>100, 27, 14, 13 and 10 μM, respectively). It becomes apparent that the criteria relating to favorable ClogP value range maybe the sole predicting factor for cytotoxic activity. More interestingly, the biological inefficacy of the inactive compounds **1a**, **1d** and **1e** (Fig. 2) could be attributed to the difficulty to cross the biological membranes due to their physicochemical properties which prevent their access to the putative binding cavity [21]. It is noteworthy to say that the structural similarity among these series was responsible for similar biological activity as evident from the experimental data (Table 5) as for example the molecular volume of the most active compounds was higher than 800 $Å^3$ while that of the inactive species was lower than 600 $Å^3$.

3. Experimental

Melting points were recorded on a Fisher–Johns apparatus (°C, uncorrected). IR spectra (KBr) were recorded on a JASCO IR Report-100 spectrophotometer (ν in cm^{-1}) and ^1H NMR spectra on a JEOL ALPHA 500 MHz and Varian XL-200 MHz

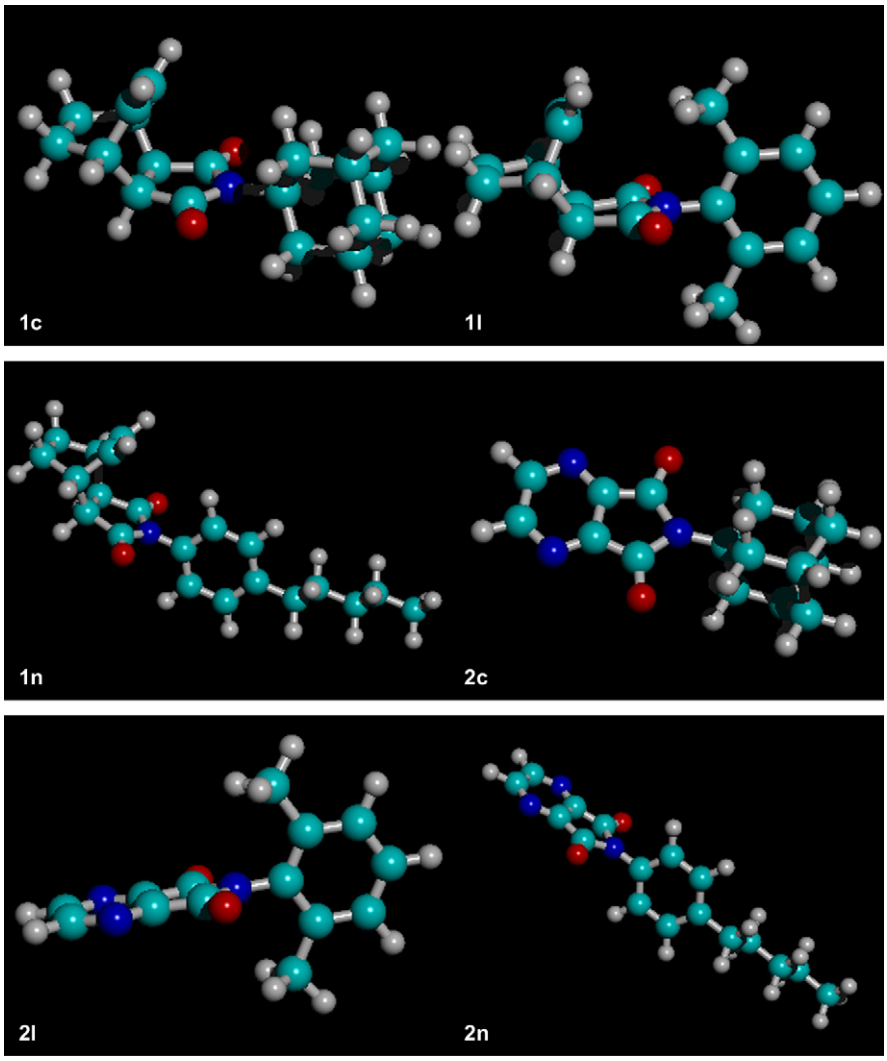

Fig. 3. Lowest energy conformers of the most active compounds **1c**, **1l**, **1n**, **2c**, **2l** and **2n** with balls and cylinders rendering.

spectrometers using TMS as internal standard (chemical shift, δ ppm). Microanalytical data (C, H, N) agreed with the proposed structures within ±0.4% of the theoretical values. All solvents were distilled before use. All reactions were run under nitrogen atmosphere. The following materials and instruments were used in biological evaluation; hemocytometer (Bright line, AO instrument Co., Buffalo, NY, USA), inverted microscope (Nikon Inc, Instrument division, Garden City, NY, USA), Dulbecco's modified Eagles medium (Gibco, Grand Island, NY, USA), supplement with 10% calf serum (Gibco), Giemsa stain (Fisher Scientific Co., Fair Lawn, NY, USA), TLC plates (RP-18F_{254}; 0.25 mm, Merck), DNA (calf thymus type I, Sigma, 100 μg/ml), DNA/methyl green (Sigma, St. Louis, MO, USA).

3.1. General and typical procedure for DPPOx-promoted synthesis of N-substituted imides

The DPPOx (1.5 equiv) was added to the equimolar solution of a carboxylic acid anhydride or imide and a primary amine in MeCN in addition to Et_3N (1.5 equiv) and the mixture was stirred at 40 °C for 15–60 min. After removal of the solvent, the residue was taken up in organic solvent such as EtOAc, and washed successively with HCl aq and $NaHCO_3$ aq. Evaporation of the dried organic solvent gave the imide which was further purified by chromatography on silica gel or by recrystallization (Tables 1 and 2). The reported compounds, including series **1** (**1a**, **1e**, **1k** and **1o**), **2** (**2a**, **2b**, **2d**, **2e**, **2k**, **2l**, **2o** and **1p**), **3** (**3a**, **3b**, **3d**, **3e**, **3f**, **3h**, **3i**, **3j**, **3k**, **3l**, **3o** and **3p**) and **4** (**4c**, **4d**, **4e**, **4i**, **4k** and **4m**), were identical with authentic samples by melting points, TLC and NMR determinations [23].

*3.1.1. Compound **1b***

Mp 121–122 °C (EtOH). ^{1}H NMR ($CDCl_3$, 500 MHz): δ 6.08–6.04 (dd, 2H, $J = 3.2$, 1.3 Hz), 3.14–3.13 (d, 2H, $J = 1.4$ Hz), 2.83 (s, 2H), 1.61–1.56 (t, 2H, $J = 1.4$ Hz), 1.40–1.38 (t, 2H, $J = 1.6$ Hz), 1.42 (s, 9H). Anal. Calcd for $C_{14}H_{19}NO_2$: 72.07, 8.21, 6.00. Found: 71.88, 8.37, 5.94.

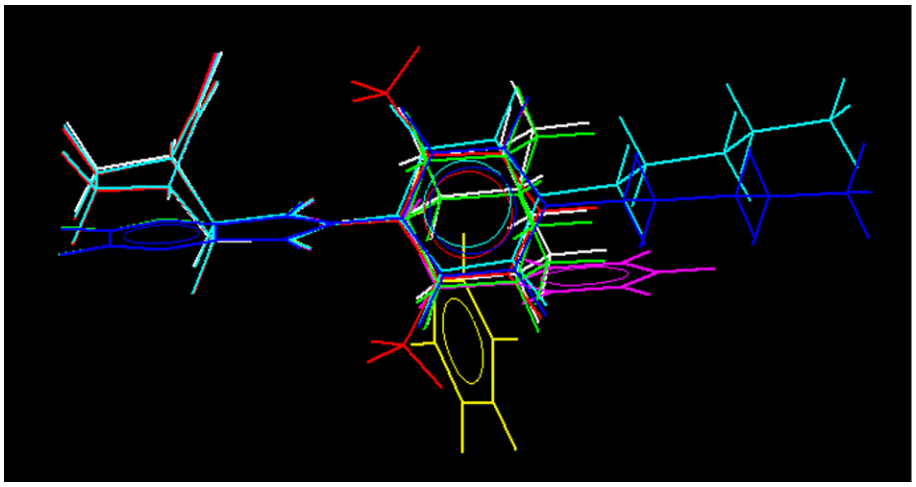

Fig. 4. Overlay of the selected active compounds and nonactive one showing the importance of the T-shaped structure for biological activity; **1c** colors white, **1d** colors violet, **1e** colors yellow, **1l** colors red, **1n** colors cyan, **2c** colors green, **2l** colors blue, T-shaped imides **1** was out of the plane of planar imides **2**. (For interpretation of the references to color in this figure legend, the reader is referred to the web version of this article.)

*3.1.2. Compound **1c***

Mp 199–200 °C (EtOH). ^{1}H NMR ($CDCl_3$, 500 MHz): δ 6.21–6.18 (dd, 2H, $J = 3.4$, 1.6 Hz), 2.72–2.70 (d, 2H, $J = 1.4$ Hz), 2.87 (s, 2H), 2.04 (s, 4H), 1.78 (s, 4H), 1.66 (s, 4H), 1.63–1.58 (t, 2H, $J = 1.3$ Hz), 1.55–1.53 (d, 3H, $J = 12$ Hz), 1.43–1.39 (t, 2H, $J = 1.6$ Hz). Anal. Calcd for $C_{20}H_{25}NO_2$: 77.14, 8.09, 4.50. Found: 77.00, 8.15, 4.40.

*3.1.3. Compound **1d***

Mp 81–82 °C (EtOH). ^{1}H NMR ($CDCl_3$, 200 MHz): δ 7.45–7.39 (m, 5H), 6.11–6.07 (dd, 2H, $J = 3.4$, 1.2 Hz), 4.85 (s, 2H), 3.46 (s, 2H), 3.17–3.15 (d, 2H, $J = 1.3$ Hz), 2.85 (s, 2H), 1.63–1.59 (t, 2H, $J = 1.3$ Hz), 1.42–1.39 (t, 2H, $J = 1.4$ Hz). Anal. Calcd for $C_{18}H_{19}NO_2$: 76.84, 6.81, 4.98. Found: 76.69, 6.84, 4.90.

*3.1.4. Compound **1f***

Mp 165–166 °C (EtOH). ^{1}H NMR ($CDCl_3$, 200 MHz): δ 6.98–6.96 (d, 2H, $J = 8.8$ Hz), 6.72–6.70 (d, 2H, $J = 8.8$ Hz), 6.00–5.96 (dd, 2H, $J = 3.4$, 1.4 Hz), 4.76 (s, 2H), 3.81 (s, 3H), 3.19–3.17 (d, 2H, $J = 1.6$ Hz), 2.81 (s, 2H), 1.61–1.57 (t, 2H, $J = 1.4$ Hz), 1.40–1.37 (t, 2H, $J = 1.6$ Hz). Anal. Calcd for $C_{18}H_{19}NO_3$: 72.71, 6.44, 4.71. Found: 72.96, 6.21, 4.57.

*3.1.5. Compound **1g***

Mp 170–171 °C (EtOH). ^{1}H NMR ($CDCl_3$, 500 MHz): δ 7.22 (s, 1H), 7.14–7.12 (d, 1H, $J = 8.0$ Hz), 7.01–6.99 (d, 1H, $J = 8.0$ Hz), 6.13–6.11 (d, 2H, $J = 3.6$ Hz), 4.84 (s, 2H), 3.81 (s, 3H), 3.79 (s, 3H), 3.21–3.19 (d, 2H, $J = 1.4$ Hz), 2.85 (s, 2H), 1.64–1.60 (t, 2H, $J = 1.3$ Hz), 1.43–1.38 (t, 2H, $J = 1.6$ Hz). Anal. Calcd for $C_{19}H_{21}NO_4$: 69.71, 6.47, 4.28. Found: 69.69, 6.51, 4.32.

*3.1.6. Compound **1h***

Mp 120–121 °C (EtOH). ^{1}H NMR ($CDCl_3$, 500 MHz): δ 7.46–7.43 (d, 2H, $J = 8.7$ Hz), 7.29–7.27 (d, 2H, $J = 8.6$ Hz), 6.12–6.10 (d, 2H, $J = 3.3$ Hz), 4.80 (s, 2H), 3.20–3.18 (d, 2H, $J = 1.3$ Hz), 2.79 (s, 2H), 1.60–1.56 (t, 2H, $J = 1.4$ Hz), 1.39–1.36 (t, 2H, $J = 1.3$ Hz). Anal. Calcd for $C_{17}H_{16}ClNO_2$: 67.66, 5.34, 4.64. Found: 67.42, 5.30, 4.61.

*3.1.7. Compound **1i***

Mp 173–174 °C (EtOH). ^{1}H NMR ($CDCl_3$, 500 MHz): δ 7.30–7.21 (m, 5H), 6.16–6.14 (d, 2H, $J = 3.6$ Hz), 5.43–5.41 (q, 1H, $J = 7.6$ Hz), 3.25–3.21 (d, 2H, $J = 3.2$ Hz), 2.87 (s, 2H), 1.81–1.79 (d, 3H, $J = 7.6$ Hz), 1.64–1.60 (t, 2H, $J = 1.6$ Hz), 1.40–1.37 (t, 2H, $J = 1.6$ Hz). Anal. Calcd for $C_{18}H_{19}NO_2$: 76.84, 6.81, 4.98. Found: 76.99, 7.01, 5.11.

*3.1.8. Compound **1j***

Mp 166–167 °C (EtOH). ^{1}H NMR ($CDCl_3$, 500 MHz): δ 7.32–7.25 (m, 5H), 6.18–6.16 (d, 2H, $J = 3.4$ Hz), 5.45–5.43 (q, 1H, $J = 7.3$ Hz), 3.27–3.24 (d, 2H, $J = 3.1$ Hz), 2.86 (s, 2H), 1.80–1.78 (d, 3H, $J = 7.7$ Hz), 1.62–1.59 (t, 2H, $J = 1.6$ Hz), 1.41–1.39 (t, 2H, $J = 1.4$ Hz). Anal. Calcd for $C_{18}H_{19}NO_2$: 76.84, 6.81, 4.98. Found: 76.71, 6.69, 4.86.

*3.1.9. Compound **1l***

Mp 216–217 °C (AcOH). ^{1}H NMR ($CDCl_3$, 500 MHz): δ 6.98–6.97 (d, 2H, $J = 7.9$ Hz), 6.87 (s, 1H), 6.09–6.05 (d, 2H, $J = 3.7$ Hz), 3.13–3.10 (d, 2H, $J = 1.7$ Hz), 2.81 (s, 2H), 2.21 (s, 6H), 1.63–1.61 (t, 2H, $J = 1.6$ Hz), 1.41–1.38 (t, 2H, $J = 1.7$ Hz). Anal. Calcd for $C_{18}H_{19}NO_2$: 76.84, 6.81, 4.98. Found: 76.70, 6.99, 4.82.

*3.1.10. Compound **1m***

Mp 243–244 °C (AcOH). ^{1}H NMR ($CDCl_3$, 500 MHz): δ 7.15–7.12 (d, 2H, $J = 6.8$ Hz), 7.01 (s, 1H), 6.24–6.22 (d, 2H, $J = 3.1$ Hz), 3.23–3.21 (d, 2H, $J = 1.5$ Hz), 3.11–3.03 (m, 2H), 2.90 (s, 2H), 1.66–1.64 (t, 2H, $J = 1.7$ Hz), 1.45–1.32 (t, 2H, $J = 1.7$ Hz), 1.23–1.20 (d, 12H, $J = 7.2$ Hz). Anal. Calcd for $C_{22}H_{27}NO_2$: 78.30, 8.06, 4.15. Found: 78.35, 7.97, 4.23.

*3.1.11. Compound **1n***

Mp 128–129 °C (EtOH). ^{1}H NMR ($CDCl_3$, 500 MHz): δ 7.61–7.59 (d, 2H, $J = 7.7$ Hz), 7.43–7.40 (d, 2H, $J = 7.6$ Hz), 6.13–6.11 (d, 2H, $J = 3.4$ Hz), 3.19–3.16 (d, 2H, $J = 3.2$ Hz), 3.11–3.03 (m, 2H), 2.79 (s, 2H), 2.31–2.29 (t, 2H, $J = 4.4$ Hz), 1.62–1.59 (t, 2H, $J = 1.4$ Hz), 1.56–1.51 (m, 2H), 1.39–1.37 (t, 2H, $J = 1.6$ Hz), 1.23–1.18 (m, 2H), 1.03–1.00 (t, 3H, $J = 4.8$ Hz). Anal. Calcd for $C_{21}H_{25}NO_2$: 77.98, 7.79, 4.33. Found: 78.04, 8.00, 4.41.

*3.1.12. Compound **1p***

Mp 116–117 °C (EtOH). ^{1}H NMR ($CDCl_3$, 500 MHz): δ 7.63–7.61 (d, 2H, $J = 8.0$ Hz), 7.42–7.40 (d, 2H, $J = 8.0$ Hz), 6.31–6.29 (dd, 2H, $J = 3.2$, 1.6 Hz), 3.27 (s, 2H), 3.04–3.03 (d, 2H $J = 1.2$ Hz), 1.69–1.67 (d, 2H, $J = 1.2$ Hz), 1.47–1.44 (d, 2H, $J = 1.6$ Hz). Anal. Calcd for $C_{17}H_{14}F_3NO_2$: 63.55, 4.39, 4.36. Found: 63.69, 4.52, 4.43.

*3.1.13. Compound **2c***

Mp 241–242 °C (AcOH). ^{1}H NMR (DMSO-d_6, 500 MHz): δ 8.50 (s, 1H), 8.44 (s, 1H), 2.02 (s, 4H), 1.76 (s, 4H), 1.64 (s, 4H), 1.59–1.56 (d, 3H, $J = 12.0$ Hz). Anal. Calcd for $C_{16}H_{17}N_3O_2$: 67.83, 6.05, 14.83. Found: 68.00, 6.15, 14.70.

*3.1.14. Compound **2f***

Mp 149–150 °C (EtOH). ^{1}H NMR ($CDCl_3$, 500 MHz): δ 8.42 (s, 2H), 7.43–7.41 (d, 2H, $J = 8.0$ Hz), 6.98–6.96 (d, 2H, $J = 8.0$ Hz), 4.81 (s, 2H), 3.74 (s, 3H). Anal. Calcd for $C_{14}H_{11}N_3O_3$: 62.45, 4.12, 15.61. Found: 62.51, 4.10, 15.73.

*3.1.15. Compound **2g***

Mp 183–184 °C (EtOH). ^{1}H NMR ($CDCl_3$, 500 MHz): δ 8.91 (s, 2H), 7.26 (s, 1H), 7.08–6.06 (d, 1H, $J = 8.0$ Hz), 6.82–6.80 (d, 1H, $J = 8.1$ Hz), 4.91 (s, 2H), 3.88 (s, 3H), 3.85 (s, 3H). Anal. Calcd for $C_{15}H_{13}N_3O_4$: 60.20, 4.38, 14.04. Found: 60.16, 4.42, 14.21.

*3.1.16. Compound **2h***

Mp 251–252 °C (AcOH). ^{1}H NMR (DMSO-d_6, 500 MHz): δ 8.98 (s, 2H), 7.58–7.56 (d, 2H, $J = 8.2$ Hz), 7.23–7.21 (d, 2H, $J = 8.4$ Hz), 5.01 (s, 2H). Anal. Calcd for $C_{13}H_8ClN_3O_2$: 57.05, 2.95, 15.35. Found: 57.10, 3.06, 15.46.

*3.1.17. Compound **2i***

Mp 173–174 °C (EtOH). ^{1}H NMR ($CDCl_3$, 500 MHz): δ 8.74 (s, 2H), 7.10–6.86 (m, 5H), 5.13–5.09 (q, 1H, $J = 7.1$ Hz), 1.69–1.67 (d, 3H, $J = 7.3$ Hz). Anal. Calcd for $C_{14}H_{11}N_3O_2$: 66.40, 4.38, 16.59. Found: 66.35, 4.50, 16.39.

*3.1.18. Compound **2j***

Mp 180–181 °C (AcOH). ^{1}H NMR ($CDCl_3$, 500 MHz): δ 8.78 (s, 2H), 7.09–6.87 (m, 5H), 5.12–5.09 (q, 1H, $J = 7.2$ Hz), 1.70–1.68 (d, 3H, $J = 7.1$ Hz). Anal. Calcd for $C_{14}H_{11}N_3O_2$: 66.40, 4.38, 16.59. Found: 66.29, 4.36, 16.43.

*3.1.19. Compound **2m***

Mp 262–263 °C (AcOH). ^{1}H NMR (DMSO-d_6, 500 MHz): δ 8.91 (s, 2H), 7.01–6.99 (d, 2H, $J = 7.7$ Hz), 6.90 (s, 1H), 3.09–32.94 (m, 2H), 1.17–1.15 (d, 12H, $J = 6.9$ Hz). Anal. Calcd for $C_{18}H_{19}N_3O_2$: 69.88, 6.19, 13.58. Found: 69.76, 6.06, 13.47.

*3.1.20. Compound **2n***

Mp 197–198 °C (MeCN). ^{1}H NMR ($CDCl_3$, 500 MHz): δ 8.76 (s, 2H), 7.36–7.34 (d, 2H, $J = 7.1$ Hz), 7.28–7.26 (d, 2H, $J = 7.7$ Hz), 2.46–2.43 (t, 2H, $J = 4.6$ Hz), 1.49–1.43 (m, 2H), 1.19–1.14 (m, 4H), 1.00–0.97 (t, 3H, $J = 4.6$ Hz). Anal. Calcd for $C_{17}H_{17}N_3O_2$: 69.14, 5.80, 14.23. Found: 70.01, 5.97, 14.38.

*3.1.21. Compound **3c***

Mp 151–152 °C (MeOH). ^{1}H NMR (DMSO-d_6, 200 MHz): δ 8.91–8.87 (m, 3H), 1.97 (s, 4H), 1.69 (s, 4H), 1.60 (s, 4H), 1.56–1.53 (s, 3H). Anal. Calcd for $C_{17}H_{18}N_2O_2$: 72.32, 6.43, 9.92. Found: 72.11, 6.36, 10.09.

*3.1.22. Compound **3g***

Mp 140–141 °C (EtOH). ^{1}H NMR ($CDCl_3$, 500 MHz): δ 9.02–8.97 (m, 3H), 7.35 (s, 1H), 6.89–6.87 (d, 1H, $J = 7.2$ Hz), 6.79–6.77 (d, 1H, $J = 7.1$ Hz), 4.51 (s, 2H), 3.67 (s, 3H), 3.37 (s, 3H). Anal. Calcd for $C_{16}H_{14}N_2O_4$: 64.42, 4.73, 9.39. Found: 64.40, 4.57, 9.26.

*3.1.23. Compound **3m***

Mp 212–213 °C (MeCN). ^{1}H NMR (DMSO-d_6, 500 MHz): δ 8.84–8.80 (m, 3H), 6.97–6.901 (m, 3H), 3.12–3.07 (m, 2H), 1.11–1.08 (d, 12H, $J = 7.9$ Hz). Anal. Calcd for $C_{19}H_{20}N_2O_2$: 74.00, 6.54, 9.08. Found: 73.89, 6.46, 9.00.

*3.1.24. Compound **3n***

Mp 179–180 °C (MeCN). ^{1}H NMR ($CDCl_3$, 500 MHz): δ 8.93–8.87 (m, 3H), 7.43–7.41 (d, 2H, $J = 7.0$ Hz), 7.35–7.32 (d, 2H, $J = 7.2$ Hz), 2.40–2.37 (t, 2H, $J = 3.9$ Hz), 1.42–1.36 (m, 2H), 1.20–1.16 (m, 4H), 0.98–0.96 (t, 3H, $J = 4.0$ Hz). Anal. Calcd for $C_{18}H_{18}N_2O_2$: 73.45, 6.16, 9.52. Found: 73.29, 6.04, 9.49.

3.2. Biological assay

3.2.1. Cytotoxicity assay

3.2.1.1. Sample and culture preparation. Samples were prepared for assay by dissolving in 50 ml of DMSO and diluting aliquots into sterile culture medium at 0.4 mg/ml. These solutions were subdiluted to 0.02 mg/ml in sterile medium and the two solutions were used as stocks to test samples at 500, 300, 200, 100, 50, 20, 10, 5, 2, and 1 μM in triplicate in the wells of microtiter plates. Vero African green monkey kidney cells were purchased from Viromed Laboratories, Minnetonka, MN, and grown in Dulbecco's modified Eagle's medium supplemented with 10% (v/v) calf serum (HyClone Laboratories, Ogden, UT), 60 mg/ml penicillin G and 100 mg/ml

streptomycin sulfate maintained at 37 °C in a humidified atmosphere containing about 15% (v/v) CO_2 in air. All components in the medium were obtained from Sigma Chemical Co., St. Louis, MO, unless otherwise indicated. Vero stocks were maintained at 34 °C in culture flasks filled with medium supplemented with 1% (v/v) calf serum. Subcultures for cytotoxicity screening were grown in the wells of microtiter trays (Falcon Microtest III 96-wells trays, Becton Dickinson Labware, Lincolin Park, NJ) by suspending Vero cells in medium following trypsin–EDTA treatment, counting the suspension with a hemocytometer, diluting in medium containing 10% calf serum to 2×10^4 cells per 200 ml culture, aliquoting into each well of a tray and culturing until confluent.

3.2.1.2. Procedure. Microtiter trays with confluent monolayer cultures of Vero cells were inverted, the medium shaken out, and replaced with serial dilutions of sterile extracts in triplicate in 100 μl medium followed by titered virus in 100 μl medium containing 10% (v/v) calf serum in each well. In each tray, the last row of wells was reserved for controls that were not treated with compounds. The trays were cultured for 48 h. The trays were inverted onto a pad of paper towels, the remaining cells rinsed carefully with medium, and fixed with 3.7% (v/v) formaldehyde in saline for at least 20 min. The fixed cells were rinsed with water, and examined visually. Cytotoxic activity is identified as confluent, relatively unaltered monolayers of stained Vero cells treated with compounds. Cytotoxicity was estimated as the concentration that caused approximately 50% loss of the monolayer.

3.2.2. DNA binding affinity

3.2.2.1. DNA binding assay. Analysis of the DNA binding affinity of the tested compounds was performed using RP-TLC plates (RP-18 F_{254}; 0.25 mm; Merck). TLC plates were pre-developed with MeOH–H_2O (8:2). Test compounds were then applied (5 mg/ml in MeOH) at the origin, followed by the addition of DNA (1 mg/ml in H_2O and MeOH mixture) at the same positions at the origin. The plates were then developed with the same solvent system and the position of the DNA was determined by spraying with anisaldehyde reagent. The reagent yields a blue color spot with DNA, and the intensity of the color was proportional to the quantity of DNA added to the plate. Ethidium bromide was used as positive control.

3.2.2.2. Methyl green/DNA displacement assay. DNA/methyl green (20 mg, Sigma, St. Louis, MO, USA) was suspended in 100 ml of 0.05 M Tris/HCl buffer, pH 7.5, containing 7.5 μM $MgSO_4$ and stirred at 37 °C with a magnetic stirrer for 24 h. Unless otherwise indicated, samples to be tested were dissolved in EtOH in Eppendorff tubes. Solvent was removed under vacuum and 200 μl of the DNA/methyl green solution was added to each tube. The absorption maxima for the DNA/methyl green complex is at 642–645 nm. Samples were incubated in the dark at ambient temperature and after 24 h the final absorbance of samples was determined. Readings were corrected for initial absorbance and normalized as a percentage of the untreated DNA/methyl green absorbance value and C_{50} were determined for each compound. Daunomycin was used as a positive control.

3.2.3. Apoptosis technique

3.2.3.1. Preparation of blood neutrophils. Neutrophils (>98% pure on May-Giemsa stain) were isolated from peripheral blood of normal healthy volunteer donors and from oesteoarthritic and rheumatoid arthritic patients by a combination of dextran sedimentation and centrifugation through discontinuous plasma percoll gradients as described by Haslett [24]. In brief, neutrophils were prepared as follows: freshly drawn venous blood was citrated (1.1 ml of 3.8% sodium citrate to 10 ml blood), centrifuged at 3000*g* for 20 min at 20 °C and the platelet rich plasma aspirated and centrifuged at 2500*g* for 10 min [for production of platelet poor plasma (PPP)] or recalcified by adding 20 μM final concentration of calcium chloride to prepare platelet rich plasma derived serum (PRPDS). To red and white cells remaining in each tube 5 ml of 6% dextran (500,000 mol wt) in 0.9% saline mixed gently and then allowed to stand for erythrocyte sedimentation for 30 min. The leukocyte-rich plasma was aspirated, centrifuged at 275g for 6 min, suspended in 2 ml. The leukocytes were then mixed with 2 ml of 42% percol (9:1 v/v percol–0.9% saline) in PPP followed by adding 2 ml of 51% percol in PPP. The gradients were centrifuged at 275g for 10 min and neutrophils were then aspirated from the interface of the 51% and 42% percol.

3.2.3.2. Culture of neutrophils. Neutrophils were prepared as described above, then resuspended in an appropriate volume of RPMI 1640 medium with 10% autologous PRPDS, 100 μg/ml of penicillin and streptomycin and then divided into five equal volumes each put in culture tube. Cells were incubated (37 °C in a 5% carbon dioxide) as follows: (1) Only cells; (2) Cells and DMSO at 0.01% v/v; (3) Cells and each compound in DMSO at dose of 50 μM culture. The age of neutrophils in culture was calculated at the start of culture at time zero (or base line), 24 h, 48 h and 72 h.

3.2.3.3. Assessment of cell viability. At time zero and at subsequent times, cells were removed from culture and counted on a hemocytometer. Cell viability was determined by trypan blue dye exclusion test; one volume of trypan blue (0.4% GiBCo) was added to five volumes of cells at room temperature for 5 min.

3.2.3.4. Measurements of apoptosis

3.2.3.4.1. Morphological assessment of apoptosis (Giemsa and Acridine orange stains). At time zero and at subsequent times, cells were removed from each culture, fixed in methanol, harvested on slides and slides were stained with May Grunwald Giemsa and examined by oil immersion light microscope. For assessment of the percentage of cells showing morphology of apoptosis 500 cells/slide were examined for each case at different times (0, 24, 48, and 72 h) in the presence or absence of the drugs used. Neutrophils were considered apoptotic if they

exhibited the highly characteristic morphological features of chromatin aggregation, nuclear pyknosis and cytoplasmic vaculation [17]. The apoptotic neutrophils' percentage at different times was calculated for normal, oesteoarthritic and rheumatoid arthritis in the presence or after addition of natural products and the results were then compared statistically using *F*-test and Students *t*- test. One drop from cell suspension was added to one drop of AO solution (10 μg/ml in PBS), mixed gently on a slide, and immediately examined with an Olympus HB-2 microscope with fluorescence attachment. Green fluorescence was detected between 500 and 525 nm. Cells exhibiting bright green fluorescent condensed nuclei (intact or fragmented) were interpreted as apoptotic cells.

3.2.3.4.2. DNA fragmentation assay. Assessment of chromatin fragmentation in neutrophils was done by modification of methods previously used for thymocytes [25]. Cells (2.5X10.7) were washed three times and resuspended in 0.15 M of NaCl solution. The cells were chilled at 4 °C and lyzed by adding 4.5 ml of 10 mM of Tris/HCl buffer (pH 8.0) containing 100 mM of EDTA and 0.2% v/v Triton X-100 (lysis buffer). After 4 h, the lysate was centrifuged at 3500*g* at 4 °C for 20 min. The supernatants were collected into tubes and precipitated with 0.1 volume of 5 M of NaCl and two volumes of absolute ethanol. The DNA was precipitated for 24 h at 4 °C. The precipitate was centrifuged at 12,500*g* at 6 °C for 15 min. The pellet was resuspended in 1 ml of 10 mM of Tris/HCl buffer (pH 8.0) containing 100 mM of EDTA and 0.1 mM of sodium dodecyl sulfate. Proteinase K was added to a final concentration of 20 mg/ml, and the sample was incubated for a further 24 h at 37 °C. The DNA was extracted with phenol and chloroform and reprecipitated with absolute ethanol. The pellet was redissolved in 20 μl of lyses buffer and 10 ml of RNase. Each sample of the purified DNA (20 μl) was subjected to electrophoresis in 1% agarose gel containing 200 μg/ml ethidium bromide and were visualized under ultraviolet light. The size of the fragments was confirmed by reference to a 1-Kb DNA ladder (Gibco/BRL). Aging neutrophils exhibit morphological features of apoptosis as nuclear pyknosis, chromatin condensation and cytoplasmic vaculation by light microscope. A bright green-fluorescent condensed nuclei (intact or fragmented), reduction of cell volume, were interpreted as apoptotic cells and expressed as a percentage of the total cell number by fluorescent microscopy. Viable cells were interpreted as cells, which exhibited a green, diffusely stained intact nucleus.

3.2.3.4.3. Chromatin fragmentation. Classical 180–200 base pair integer oligonucleosome ''ladder'' was observed by using gel electrophoresis of the extracted DNA as a typical degeneration pattern of apoptosis. This confirms the previously obtained results from morphological assessment.

3.3. Molecular modeling

Initial structures for the molecules **1c**, **1d**, **1e**, **1l**, **1n**, **2c**, **2l** and **2n** were constructed using the HyperChem program version 5.1. The MM+ [19] (calculations in vacuo, bond dipole option for electrostatics, Polak–Ribiere algorithm, and RMS gradient of 0.01 kcal/Å mol) conformational searching in torsional space was performed using the multiconformer method [26]. Energy minima for compounds **1c**, **1d**, **1e**, **1l**, **1n**, **2c**, **2l** and **2n** were determined by a semi-empirical method AM1 [27] (as implemented in HyperChem 5.1). The conformations thus obtained were confirmed as minima by vibrational analysis. Atom-centred charges for each molecule were computed from the AM1 wave functions (HyperChem 5.1) by the procedure of Orozco and Luque [28], which provides derived charges that closely resemble those obtainable from ab initio 6-31G* calculations.

4. Conclusion

We successfully developed an efficient, economical and practical method for the synthesis of a wide range of imide derivatives by using inexpensive and readily available reagents under mild conditions. In light of its operational simplicity, simple purification procedure, and high efficiency, the procedure is expected to have broad utility, especially in the synthesis of functionalized imide derivatives, for future biological and chemical applications. Based on a general pattern inspired by the reference literature, we have completed biological evaluation of the target compounds as potential cytotoxic, DNA binder and apoptosis inducers. These compounds were performed in a cytotoxicity in vitro assay against Vero African green monkey kidney cells. Some compounds showed good cytotoxic activity against the cell line tested, with IC_{50} values in the low medium micro-molar range. Compounds which showed cytotoxicity were evaluated in a DNA binding and apoptosis assay. Some compounds exhibited high DNA affinity and ability in inducing apoptosis in the cell line tested. The best DNA affinity and apoptosis levels were achieved for compounds **1n**, **2n**, **3n**, **1l**, **2l**, **3l**, **1c**, **2c** and **3c**. Although a precise structure–activity relationship can not be defined, it is possible to point out some general tendencies observed for the active compounds, the greatest DNA binding and apoptotic activity is found in compounds with a nonplanar imide nucleus. With regard to the N-functional group of connection, the best results were obtained for the 4-pentylphenyl, 1-adamantyl, and 2,6-dimethylphenyl groups. In general, a direct relationship has been found between the apoptotic activity and the cytotoxicity, while the affinity for DNA was partially correlated with cytotoxic activity, thereby suggesting the existence of two different mechanisms of action controlling cytotoxic activity.

Acknowledgement

The author would like to thank Prof. Farid Badria (Department of Pharmacognosy, Faculty of Pharmacy, Mansoura University, Egypt) for providing the biological data.

References

[1] (a) M.E. Salvati, A. Balog, W. Shan, D.D. Wei, D. Pickering, R.M. Attar, J. Geng, C.A. Rizzo, M.M. Gottardis, R. Weinmann, S.R. Krystek, J. Sack, Y. An, K. Kish, Bioorg. Med. Chem. Lett. 15 (2005) 271;
(b) J. Kossakowski, M. Jarocka, Il Farmaco 56 (2001) 785;

(c) K. Ishizumi, A. Kojma, F. Antoku, Chem. Pharm. Bull. 39 (1991) 2288;
(d) Y. Sabata, M. Shichita, K. Sasaki, Y. Hashimoto, S. Iwasaki, Chem. Pharm. Bull. 43 (1995) 177;
(e) D.P. Jindal, V. Bedi, B. Jit, N. Karkra, S. Guleria, R. Bansal, A. Palusczak, R.W. Hartmann, Il Farmaco 60 (2005) 283;
(f) J.J. Wang, S.S. Wang, C.F. Lee, M.A. Chung, Y.T. Chern, Chemotherapy 43 (1997) 182;
(g) A.L. Machado, L.M. Lima, J.X. Araújo Jr., C.A.M. Fraga, V.L.G. Koatz, E.J. Barreiro, Bioorg. Med. Chem. Lett. 15 (2005) 1169;
(h) S. Kenji, N. Hideko, U. Yoshihiro, S. Yoshikazu, N. Kazuharu, W. Motoji, W. Konstanty, T. Tadafumi, A. Tetsuji, Y. Yuji, K. Kenji, H. Hitoshi, Bioorg. Med. Chem. 13 (2005) 4014;
(i) A. Mayer, S. Neuenhofer, Angew. Chem. Int. Ed. Engl. 33 (1994) 1044;
(j) F.B. Miguel, D. Gema, S. Beatriz, R. Cynthia, R. Simmon, B. Teresa, Eur. J. Med. Chem. 37 (2002) 541;
(k) H. Miyachi, A. Azuma, A. Ogasawara, E. Uchimura, N. Watanabe, Y. Kobayashi, F. Kato, M. Kato, H. Hashimoto, J. Med. Chem. 40 (1997) 2858.

[2] (a) M.A. Walker, J. Org. Chem. 60 (1995) 5352; Tetrahedron Lett. 35 (1994) 665;
(b) R.L. Dorta, C.G. Francisco, E. Suárez, Tetrahedron Lett. 35 (1994) 1083.

[3] A. Da Settimo, G. Primofiore, F. Da Settimo, F. Simorini, C. La Motta, A. Martinelli, E. Boldrini, Eur. J. Med. Chem. 31 (1996) 49.

[4] N.B. Mehta, A.P. Phillips, F.F. Lui, R.E. Brooks, J. Org. Chem. 25 (1960) 1012.

[5] P.Y. Reddy, S. Kondo, T. Toru, Y. Ueno, J. Org. Chem. 62 (1997) 2652.

[6] A.K. Bose, M.S. Manhas, M. Ghush, V.S. Raju, K. Tabei, Z. Urbanczyk-Lykewaska, Heterocycles 30 (1990) 741.

[7] K.C. Westaway, R.N. Gedye, J. Microw. Power Electromagn. Energy (1995) 219.

[8] For the synthesis and application of DPPOx, see: (a) T. Kunieda, T. Higuchi, Y. Abe, M. Hirobe, Tetrahedron 39 (1983) 3253;
(b) T. Kunieda, T. Nagamatsu, T. Higuchi, M. Hirobe, Tetrahedron Lett. 29 (1988) 2203.

[9] (a) H.A. Staab, Angew. Chem. Int. Ed. Engl. 1 (1962) 351;
(b) H.C. Beyerman, W.M. Van den Brink, Rec. Trav. Chim. 80 (1961) 1372;
(c) T. Izawa, T. Mukaiyama, Chem. Lett. (1977) 1443;
(d) T. Mukaiyama, Angew. Chem. Int. Ed. Engl. 15 (1976) 94.

[10] (a) I. Antonini, P. Polucci, A. Magnano, D. Cacciamani, M.T. Konieczny, J. Paradziej-Łukowicz, S. Martelli, Bioorg. Med. Chem. 11 (2003) 399;
(b) A. Kamal, O. Srinivas, P. Ramulu, G. Ramesh, P. Praveen Kumar, M. Shiva Kumar, Bioorg. Med. Chem. 12 (2004) 4337;
(c) B.K. Banik, F.F. Becker, I. Banik, Bioorg. Med. Chem. 12 (2004) 2523;
(d) E.R. El-Bendary, F.A. Badria, Arch. Pharm. Med. Chem. 333 (2000) 99;
(e) M.A. El-Sherbeny, F.A. Badria, S.A. Kheira, Med. Chem. Res. 6 (1996) 28.

[11] (a) A. Amutha, V. Subramanian, B. Unni Nair, Chem. Phys. Lett. 344 (2001) 40;
(b) J.P. Dheyongera, W.J. Geldenhuys, T.G. Dekker, C.J. Van der Schyf, Bioorg. Med. Chem. 13 (2005) 689;
(c) W. Zhang, Y. Dai, U. Schmitz, T.W. Bruice, FEBS Lett. 509 (2001) 85;
(d) D.F.S. Kehrer, O. Soepenberg, W. Loos, J. Verweij, A. Sparreboom, Anticancer Drugs 12 (2001) 89;
(e) K. Chen, S.J. Adelstein, A.I. Kassis, J. Mol. Struct. (Theochem) 711 (2004) 49.

[12] J.M. Pezzuto, S.K. Antosiak, W.M. Messmer, M.B. Slaytor, G.R. Honig, Chem. Biol. Interact. 43 (1983) 323.

[13] J.M. Pezzuto, C.T. Che, D.D. McPherson, J.-P. Zhu, G. Topcu, C.A.J. Erdelmeier, G.A. Cordell, J. Nat. Prod. 54 (1991) 1522.

[14] N.S. Burres, A. Frigo, R.R. Rasmussen, J.B. McAlpine, J. Nat. Prod. 55 (1992) 1582.

[15] (a) Z. Huang, Chem. Biol. 9 (2002) 1059;
(b) R.A. Schlegel, P. Williamson, Cell Death Differ. 8 (2001) 551;
(c) S.J. Martin, C.P. Reutelingsperger, A.J. McGahon, J.A. Rader, R.C. Van Scie, D.M. LaFace, D.R. Green, J. Exp. Med. 182 (1995) 1545;
(d) F.R. Kerr, J. Pathol. 105 (1971) 13;
(e) F.E. Sarrol, I.D. Bowen, Cell Tissue Res. 21 (1988) 45;
(f) D.A. Carson, J.M. Ribeiro, Lancet 341 (1993) 1251;
(g) H.-Z. Zhang, J. Drewe, B. Tseng, S. Kasibhatla, S.X. Cai, Bioorg. Med. Chem. 12 (2004) 3649;
(h) H. Corwin, J. Ali, B.M. Suresh, G. Rajni, B. Benjamin, Bioorg. Med. Chem. 11 (2003) 3015.

[16] (a) K. Debatin, Toxicol. Lett. 112 (2000) 41;
(b) D.W. Nicholson, Nature 407 (2000) 810;
(c) P. Huang, A. Oliff, Trends Cell Biol. 11 (2001) 343.

[17] M.K. Pec, A. Aguirre, K. Moser-Thier, J.J. Fernandez, M.L. Souto, J. Dorta, F. Diaz-Gonzales, J. Villar, Biochem. Pharmacol. 65 (2003) 1451.

[18] G. Evan, K.H. Vousden, Nature 411 (2001) 342.

[19] (a) S. Profeta, N.L. Allinger, J. Am. Chem. Soc. 107 (1985) 1907;
(b) N.L. Allinger, J. Am. Chem. Soc. 99 (1977) 8127.

[20] HyperChem version 5.1, Hypercube Inc.

[21] S.T. Al-Rashood, I.A. Aboldahab, M.N. Nagi, L.A. Abouzeid, A.A.M. Abdel-Aziz, S.G. Abdul-hamide, K.M. Youssef, A.M. Al-Obaid, H.I. El-Subbagh, Bioorg. Med. Chem. 14 (2006) 8608.

[22] R.P. Verma, A. Kurup, C. Hansch, Bioorg. Med. Chem. 13 (2005) 237.

[23] (a) M. Ishikawa, M. Fujimoto, M. Sakai, A. Matsumoto, Chem. Pharm. Bull. 16 (1968) 622;
(b) A. Meijer, S. Otto, J.B.F.N. Engberts, J. Org. Chem. 63 (1998) 8989;
(c) M.R. Baar, K. Wustholz, J. Chem. Educ. 82 (2005) 1393;
(d) V.V. Kovalishin, I.V. Tetko, A.I. Luik, J.R. Chretien, D.J. Livingstone, Russ. J. Bioorganic Chem. 27 (2001) 267;
(e) T. Goto, M. Konno, M. Saito, R. Sato, Bull. Chem. Soc. Jpn. 62 (1989) 1205;
(f) M.M. Blanco, G.J. Levin, C.B. Schapira, I.A. Perillo, Heterocycles 57 (2002) 1881;
(g) B. Gutkowska, Z. Kabzinska, J. Wasiak, Acta Pol. Pharm. 44 (1987) 242;
(h) P.M. Harrington, Heterocycles 35 (1993) 683;
(i) T. Noguchi, H. Fujimoto, H. Sano, A. Miyajima, H. Miyachi, Y. Hashimoto, Bioorg. Med. Chem. Lett. 15 (2005) 5509.

[24] (a) J.S. Savill, A.H. Wyllie, J.E. Henson, C. Haslett, J. Clin. Invest. 83 (1989) 865;
(b) C. Haslett, M. Guthrie, M. Henson, Am. J. Pathol. 199 (1985) 101.

[25] (a) H. Wyla, Nature 284 (1980) 555;
(b) G. Maino, G. Jotris, Am. J. Pathol. 146 (1995) 3.

[26] M. Lipton, W.C. Still, J. Comput. Chem. 9 (1988) 345.

[27] M.J.S. Dewar, E.G. Zoebisch, E.F. Healy, J.J.P. Stewart, J. Am. Chem. Soc. 107 (1985) 3902.

[28] M. Orozco, F.J. Luque, J. Comput. Chem. 11 (1990) 909.